JOURNAL OF VIROLOGY, Nov. 1997, p. 8624–8631 Vol. 71, No. 11
0022-538X/97/$04.00+0
Copyright © 1997, American Society for Microbiology

VPg of Tobacco Etch Potyvirus Is a Host Genotype-Specific Determinant for Long-Distance Movement

MARY C. SCHAAD,† ANDREW D. LELLIS,† AND JAMES C. CARRINGTON*†

Department of Biology, Texas A & M University, College Station, Texas 77843

Received 13 May 1997/Accepted 4 August 1997

The V20 cultivar of *Nicotiana tabacum* was shown previously to exhibit a strain-specific restriction of long-distance movement of tobacco etch potyvirus (TEV). In V20, both TEV-HAT and TEV-Oxnard strains are capable of genome amplification and cell-to-cell movement, but only TEV-Oxnard is capable of systemic infection by vasculature-dependent long-distance movement. To investigate the basis for host-specific movement of TEV, chimeric virus genomes were assembled from TEV-HAT and TEV-Oxnard. Viruses containing the TEV-Oxnard coding regions for HC-Pro and/or capsid protein (CP), two proteins that are known to be essential for TEV long-distance movement, failed to infect V20 systemically. In contrast, chimeric viruses encoding the TEV-Oxnard VPg domain of NIa were able to infect V20 systemically. The critical region controlling the infection phenotype in V20 was mapped to a 67-nucleotide segment containing 10-nucleotide differences, but only five amino acid differences, between TEV-HAT and TEV-Oxnard. In V20 coinfection experiments, a restricted strain had no effect on systemic infection by a long-distance movement-competent chimeric strain, suggesting that the restricted strain was not inducing a generalized systemic resistance response. These data suggest that the VPg domain, which is covalently attached to the 5′ end of genomic RNA, interacts either directly or indirectly with host components to facilitate long-distance movement.

The infection of plants by viruses requires a series of compatible interactions between viral and host factors to permit genome replication at the single-cell level, cell-to-cell movement through plasmodesmata, and long-distance movement through the phloem (7). Virus-host interactions during the movement steps typically involve one or more virus-encoded movement proteins (MPs), which facilitate cell-to-cell transport of infectious material through plasmodesmata (10, 27). Long-distance movement through the phloem may be a more complex process, involving passage through plasmodesmata connecting several cell types and apparent passive transport through phloem (24). Depending on the virus, long-distance movement is regulated or affected by several viral proteins, including MP and capsid protein (CP) (7). In addition, several plant virus replication proteins are known to influence cell-to-cell or long-distance movement. For example, brome mosaic virus mutants containing deletions in the 2a protein (RNA-dependent RNA polymerase) gene are deficient in systemic spread (43). The multifunctional replication protein encoded by RNA 1 of the cucumber mosaic virus Fny strain enables more efficient cell-to-cell movement than does RNA 1 of the Sny strain in zucchini (15). Naturally occurring genetic variation affecting the p126 protein of the masked strain of tobacco mosaic virus results in defects in long-distance movement in tobacco (11, 17, 35). How MP, CP, replication proteins, and other nonstructural proteins interact to facilitate local and systemic spread in plants is understood poorly.

In contrast to most groups of plant viruses, movement functions of potyviruses are performed exclusively by proteins with other roles in encapsidation or genome replication (9, 12, 20, 21). CP is required for both cell-to-cell and long-distance movement (12, 13). The core domain of CP, which is essential for flexuous rod-shaped virion assembly, is necessary for cell-to-cell movement. The N- and C-terminal domains of CP, which are exposed on the virion surface, are required for efficient long-distance movement through phloem. Cell-to-cell movement was shown recently to also require the CI helicase protein (4a). Long-distance movement also requires, in addition to CP, one or more functions provided by helper component-proteinase (HC-Pro), a multifunctional protein also involved in aphid-mediated transmission, polyprotein processing, and genome amplification (2, 9, 20, 21). It was proposed that HC-Pro might function in movement either directly by interaction with other viral movement factors or indirectly through interaction with host factors (20).

Roles for host factors in virus movement have been inferred on the basis of genetic analyses, although the biochemical nature of such factors has yet to be identified. Strain- and virus-specific restriction of movement in plants have been described in several virus-host systems, including tobacco etch potyvirus (TEV) in tobacco (8, 37), tomato mosaic tobamovirus in tomato (29, 30, 44), cowpea chlorotic mottle bromovirus in soybean (16), and several viruses in *Arabidopsis thaliana* (4, 23, 25, 41). In some cases, restricted movement may result from elicitation of active defense responses, while in others, restricted movement may involve incompatibilities between host and virus-encoded factors necessary for efficient transit through transport pathways.

We demonstrated previously that the *Nicotiana tabacum* cultivar V20 exhibits a strain-specific defect in supporting long-distance movement of TEV (37). Immunohistochemical analyses revealed that V20 plants support cell-to-cell movement in inoculated leaves at least to the point of phloem companion cells, suggesting that the restriction occurs at the point of phloem sieve element loading or unloading. Genetic segregation analysis indicated that the TEV-restricted phenotype of V20 requires at least two recessive, unlinked loci. The V20 cultivar restricts systemic infection by most TEV strains, including TEV-HAT, but is fully susceptible to TEV-Oxnard (8, 37). In this study, the viral genetic determinant conditioning long-distance movement capability of TEV-Oxnard in V20

* Corresponding author. Phone: (509) 335-2477. Fax: (509) 335-2482. E-mail: carrington@wsu.edu.

† Present address: Institute of Biological Chemistry, Washington State University, Pullman, WA 99164-6340.

plants was identified through construction and analysis of TEV-Oxnard/TEV-HAT hybrid genomes.

MATERIALS AND METHODS

Virus strains and plants. The HAT and Oxnard strains of TEV were used to construct all viruses. All chimeric viruses were assembled by using TEV-GUS derived from pTEV7DAN-GUS as the base vector (14). TEV-GUS consists of the TEV-HAT genome (1) with the bacterial β-glucuronidase (GUS) coding sequence inserted between the P1 and HC-Pro coding regions. *N. tabacum* cultivars Xanthi nc, Havana$_{425}$, and V20 were used as indicated.

RNA extraction, reverse transcription, and PCR amplification. RNA was isolated from purified virus preparations by proteinase K-sodium dodecyl sulfate treatment followed by phenol extraction and ethanol precipitation. Reverse transcription reactions were done using an oligo(dT) or sequence-specific primer. Reactions contained 1 OD (optical density unit) of primer/ml, 0.2 mM each deoxynucleoside triphosphate (dNTP), 200 ng of RNA, and 200 U of reverse transcriptase (Superscript; Gibco BRL). Second-strand cDNA was synthesized by using 150 μM each dNTP, 2.4 U of RNase H, and 55.5 U of DNA polymerase I (Stratagene). Reaction products were extracted with phenol-chloroform and precipitated by ethanol prior to PCR amplification. Standard PCRs were performed with 2 OD of primer/ml, 80 μM each dNTP, 50 ng of DNA, 10% dimethyl sulfoxide, and 2.5 U of *Pfu* DNA polymerase (Stratagene).

Construction of chimeric viruses. To make chimeric viruses containing the Oxnard CP (TEV-GUS^{OxCP} and TEV-GUS$^{OxCP/HC}$), a *Kpn*I restriction site (GGTACC) was inserted by oligonucleotide-directed mutagenesis (22) between codons 1 and 2 of the CP coding sequence of pTEV7DAN-GUS-3′Stu. This is a full-length TEV cDNA-containing plasmid that contains a *Stu*I site at the 3′ end of the CP coding region (28). CP coding sequence from TEV-Oxnard was amplified by PCR using 5′ and 3′ primers that included *Kpn*I and *Stu*I sites, respectively, and inserted into the full-length vector.

To make the chimeras expressing the Oxnard HC-Pro (TEV-GUS^{OxHC} and TEV-GUS$^{OxCP/HC}$), a *Stu*I restriction site was inserted by oligonucleotide-directed mutagenesis at TEV nucleotide 2437, which is immediately after codon 1 of the P3 coding region in the intermediate plasmid, pTL7SN.3-1027 (19). Full-length TEV vectors containing this *Stu*I site were created by subcloning the *Kpn*I-*Hpa*I fragment into pTEV7DAN ↓ GUS HK H (19), using the engineered *Kpn*I site between the GUS and HC-Pro coding sequence and the naturally occurring *Hpa*I site at nucleotide 2681 within the P3 region. The HC-Pro sequence from TEV-Oxnard was amplified by PCR using 5′ and 3′ primers containing *Kpn*I and *Stu*I sites, respectively, and inserted into the full-length vectors.

A series of chimeric virus genomes containing sequence derived from the central region of the TEV-Oxnard genome was constructed by using naturally occurring *Sac*I (nucleotide 3603), *Bam*HI (nucleotide 5915), and *Bsu*36I (nucleotide 6517) restriction sites. TEV-GUS$^{OxSac-Bsu}$, TEV-GUS$^{OxSac-Bam}$, and TEV-GUS$^{OxBam-Bsu}$ were generated by subcloning the *Sac*I-*Bsu*36I, *Sac*I-*Bam*HI, and *Bam*HI-*Bsu*36I fragments, respectively, from TEV-Oxnard cDNA into pTEV7DAN-GUS.

A series of chimeric viruses containing various amounts of TEV-Oxnard sequence between the *Bam*HI and *Bsu*36I sites within the NIa coding region was constructed by using a recombinant PCR strategy (18). Each recombinant was generated by using a set of overlapping TEV-HAT- and TEV-Oxnard-derived PCR products, where the overlap spanned at least 26 invariant nucleotides between the *Bam*HI and *Bsu*36I sites. Both fragments from the set were gel purified and used as primer/templates in a second PCR, and the recombinant molecule was digested with *Bam*HI and *Bsu*36I and subcloned into a full-length vector. Recombinant viruses containing the following TEV-Oxnard sequences were produced: TEV-GUS$^{Ox5991-Bsu}$, nucleotides 5991 to 6517; TEV-GUS$^{Ox6050-Bsu}$, nucleotides 6050 to 6517; TEV-GUS$^{OxBam-6244}$, nucleotides 5915 to 6244; TEV-GUS$^{OxBam-6069}$, nucleotides 5915 to 6069; and TEV-GUS$^{OxBam-6000}$, nucleotides 5915 to 6000. Nucleotide sequence analysis between the *Bam*HI and *Bsu*36I sites was conducted to verify the identity of each recombinant genome.

Sequence analysis. Dideoxynucleotide sequence analysis was performed on all recombinant viruses by a cycle sequencing method (Epicentre Technologies). Nucleotide sequence and amino acid comparisons were performed with the Clustal W computer program, version 1.6 (42).

Inoculation of plants and protoplasts. In vitro synthesis of m^{7}GpppG-capped infectious transcripts by using SP6 RNA polymerase (Ambion) was described previously (14). Transcripts (approximately 10 μg) were introduced into protoplasts (7.5×10^5) by the polyethylene glycol-mediated transfection method (34). Protoplasts (2.5×10^5) were harvested at 24, 48, and 72 h postinoculation (p.i.). The cells were frozen at −80°C, thawed, and resuspended in 100 μl of GUS lysis buffer (40 mM sodium phosphate, 10 mM EDTA, 0.1% Triton X-100, 0.1% sodium lauryl sarcosine, 0.07% β-mercaptoethanol [pH 7.0]). GUS activity was measured by using the fluorometric substrate 4-methylumbelliferyl-β-D-glucuronide (4-MUG). Activity values were calculated as picomoles of substrate cleaved per minute per 10^5 protoplasts. The TEV-GUS/VNN mutant containing a replication-debilitating mutation affecting the conserved GDD motif within the NIb polymerase (26) was used as the negative genome amplification control.

Transcripts (approximately 2 μg) were also used to inoculate each of two carborundum-dusted leaves of plants. Symptomatic leaves were harvested at 5 or 6 days p.i., ground in 5 volumes of TE (10 mM Tris-HCl [pH 7.6], 1 mM EDTA), and used as inoculum in subsequent experiments. For all experiments, at least eight plants were inoculated with mutant and control viruses. At 7 days p.i., total tissue from leaves that were two nodes above the top inoculated leaf (2+ leaves) was ground in 5 volumes of GUS lysis buffer and clarified by centrifugation at 13,000 × *g* for 1 min. GUS activity was measured by using the fluorometric substrate 4-MUG. Total protein concentration was determined by the method of Bradford (3). Activity values were calculated as picomoles of substrate cleaved per minute per microgram of protein. GUS activity was also visualized in inoculated leaves after vacuum infiltration with the colorimetric substrate 5-bromo-4-chloro-3-indolyl-β-D-glucuronide (X-Gluc) at 7 days p.i. Photographs were taken with Kodak Ektachrome 160 tungsten film. The slides were scanned and digitized by using a Nikon LS-1000 Film Scanner and Adobe Photoshop 3.0 software (Adobe Systems Incorporated).

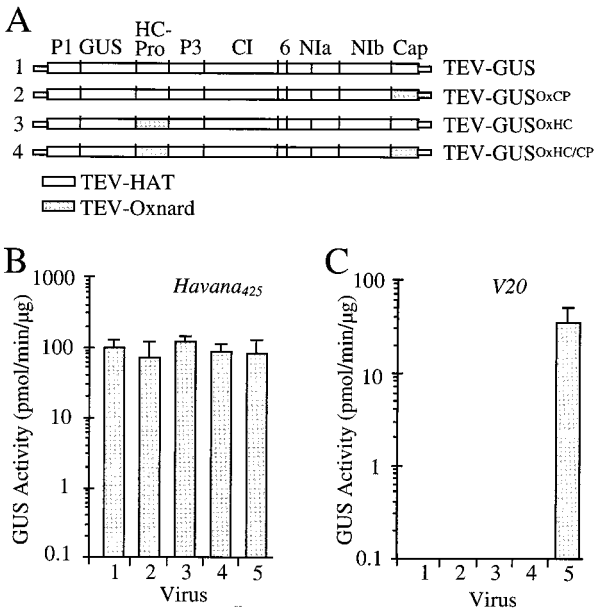

FIG. 1. (A) Diagrammatic representation of chimeric TEV genomes. 1, TEV-GUS; 2, TEV-GUS^{OxCP}; 3, TEV-GUS^{OxHC}; 4, TEV-GUS$^{OxHC-CP}$. (B and C) Systemic infection of Havana$_{425}$ (B) and V20 (C) plants by the TEV chimeras and positive control TEV-GUS$^{OxSac-Bsu}$ (columns 5; see Figure 2A). The number under each bar corresponds to the code for each virus as shown in panel A. GUS activity was quantitated in 2+ leaves at 7 days p.i. Each bar represents the mean ± standard deviation from eight plants.

Nucleotide sequence accession number. The TEV-Oxnard partial NIa sequence has been assigned GenBank accession no. AF003824.

RESULTS

CP and HC-Pro from TEV-Oxnard do not stimulate long-distance movement in V20 tobacco. The restriction of TEV-GUS (a TEV-HAT-derived virus) in V20 tobacco occurs at the level of long-distance movement (37). Infection foci form and expand in inoculated leaves, but movement to noninoculated tissues is restricted. In fact, the phenotype of TEV-GUS in V20 tobacco is very similar to the phenotype of certain TEV-GUS mutants with defects in HC-Pro or CP in susceptible varieties of tobacco, such as Havana$_{425}$ and Xanthi nc (9, 12, 13, 20, 37). We tested the hypothesis that TEV-Oxnard is able to infect V20 tobacco systemically because of one or more determinants located within the CP and/or HC-Pro sequences. Chimeric viruses containing the TEV-Oxnard CP or HC-Pro (or both) were produced (Fig. 1A). Each virus infected Havana$_{425}$ tobacco systemically, accumulating GUS activity in noninoculated tissue to levels comparable to that of TEV-GUS at 7 days p.i. (Fig. 1B, columns 1 to 4). However, GUS activity was not detected in noninoculated leaves of V20 tobacco inoculated either with TEV-GUS or with the CP or HC-Pro recombinant

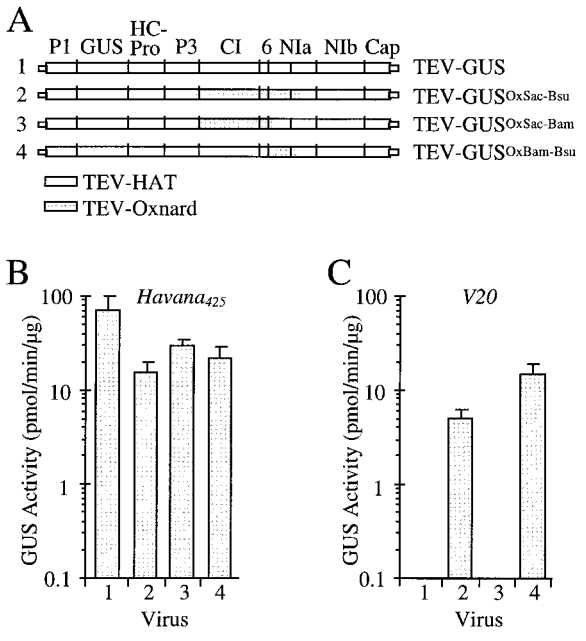

FIG. 2. (A) Diagrammatic representation of chimeric TEV genomes. 1, TEV-GUS; 2, TEV-GUS$^{OxSac-Bsu}$; 3, TEV-GUS$^{OxSac-Bam}$; 4, TEV-GUS$^{OxBam-Bsu}$. (B and C) Systemic infection of Havana$_{425}$ (B) and V20 (C) plants. The number under each bar corresponds to the code for each virus as shown in panel A. GUS activity was quantitated in 2+ leaves at 7 days p.i. Each bar represents the mean ± standard deviation from eight plants.

virus (Fig. 1C, columns 1 to 4), although each virus formed infection foci in inoculated leaves (data not shown). A recombinant virus able to move long distances in V20 plants (see below) was used as a positive control and infected both Havana$_{425}$ and V20 plants systemically (Fig. 1B and C, columns 5). These data fail to support the hypothesis that TEV-Oxnard CP and HC-Pro, alone or in combination, facilitate systemic infection of V20 tobacco.

A determinant for long-distance movement of TEV-Oxnard in V20 is located within the NIa sequence. Recombinant TEV-GUS genomes containing various segments of the central region of the TEV-Oxnard genome were assembled (Fig. 2A). In each case, the chimeric virus was subjected to a series of analyses to measure long-distance movement and genome amplification activities in both Havana$_{425}$ and V20 tobacco. Long-distance movement was assessed by measuring GUS activity in 2+ leaves and by histochemical colorimetric assay for GUS activity in inoculated leaves. In the histochemical assay in inoculated leaves, long-distance movement activity is revealed by GUS activity patterns that follow major and minor veins. TEV-GUS was used as a control in all experiments.

Unlike the chimeric viruses containing the TEV-Oxnard CP and/or HC-Pro, a recombinant virus containing the TEV-Oxnard sequence coding for part of P3, all of CI and 6-kDa protein, and part of NIa (TEV-GUS$^{OxSac-Bsu}$) was able to infect both Havana$_{425}$ and V20 tobacco systemically. Noninoculated leaves of TEV-GUS$^{OxSac-Bsu}$-infected Havana$_{425}$ and V20 tobacco exhibited GUS activity, whereas only Havana$_{425}$ plants were infected systemically by TEV-GUS (Fig. 2B and C). In this and most other experiments, the absolute level of GUS activity induced by TEV-GUS$^{OxSac-Bsu}$ in Havana$_{425}$ plants was lower than that of parental TEV-GUS (Fig. 2B). Inoculated V20 leaves containing TEV-GUS$^{OxSac-Bsu}$ contained a GUS activity pattern that revealed vasculature-dependent movement, while V20 leaves inoculated with parental TEV-GUS contained only isolated infection foci (Fig. 3).

The TEV-Oxnard sequence represented in TEV-GUS$^{OxSac-Bsu}$ was tested in two segments in recombinant viruses TEV-GUS$^{OxSac-Bam}$ and TEV-GUS$^{OxBam-Bsu}$ (Fig. 2A). TEV-GUS$^{OxSac-Bam}$-infected Havana$_{425}$ plants, but not V20 plants, systemically (Fig. 2B and C). Leaves of V20 plants inoculated with TEV-GUS$^{OxSac-Bam}$ contained isolated infection foci resembling those in TEV-GUS-inoculated V20 leaves (Fig. 3). In contrast, TEV-GUS$^{OxBam-Bsu}$ was able to infect both Havana$_{425}$ and V20 systemically (Fig. 2B and C) and to spread along the vasculature in inoculated leaves of both plants (Fig. 3). The TEV-GUS$^{OxBam-Bsu}$ recombinant virus contained TEV-Oxnard sequence derived entirely from within the NIa coding region, suggesting that the ability to spread systemically in V20 was due, at least in part, to NIa or NIa coding sequence.

It was possible that systemic infection capability of TEV-GUS$^{OxSac-Bsu}$ and TEV-GUS$^{OxBam-Bsu}$ in V20 plants was due to enhanced genome amplification levels. To test this possibility, protoplasts were prepared from Havana$_{425}$ and V20 plants and inoculated with transcripts representing parental and recombinant genomes. Genome amplification activity was determined for each virus by measuring GUS activity levels at 72 h p.i. and calculating a relative mean value based on parental TEV-GUS as the 100% standard. Additionally, TEV-GUS/VNN was used as an amplification-defective control in all experiments to reveal the level of GUS activity directed by input transcripts (26). In Havana$_{425}$ and V20 protoplasts, TEV-GUS$^{OxSac-Bsu}$, TEV-GUS$^{OxSac-Bam}$, and TEV-GUS$^{OxBam-Bsu}$ amplified to levels between 17 and 52% of that of TEV-GUS (Table 1). However, the relative amplification levels of each recombinant genome in the two protoplast types were similar (Table 1), regardless of whether the virus was able to infect V20 plants systemically. In fact, the recombinant genome with highest relative amplification level in Havana$_{425}$ and V20 protoplasts in this set of experiments (TEV-GUS$^{OxSac-Bam}$) was incapable of long-distance movement in V20 plants.

The determinant for long-distance movement of TEV-Oxnard in V20 is located within a 67-nucleotide segment of the VPg domain coding region. The TEV-GUS$^{OxBam-Bsu}$ hybrid, which was able to move long distances in V20 tobacco, contains TEV-Oxnard genome sequence between positions 5915 (*Bam*HI site) and 6517 (*Bsu*36I site). This segment encodes most of the VPg domain and a small part of the proteinase domain. The genome sequence of TEV-Oxnard between nucleotides 5692 and 6522 (NIa nucleotides 1 to 825) was determined and compared to the homologous TEV-HAT sequence (Fig. 4A). The VPg domain coding regions (NIa nucleotides 1 to 564) of TEV-HAT and TEV-Oxnard differed at 36 nucleotide positions (6% difference), resulting in 20 amino acid differences (11% difference [Fig. 4B]). Within the partial proteinase domain coding region (NIa nucleotides 565 to 825), the two strains differed at 13 nucleotide positions and 5 amino acid positions (Fig. 4B). Within the *Bam*HI-*Bsu*36I interval (NIa codons 75 to 277), changes resulting in amino acid differences were clustered in two regions. Cluster I had differences resulting in amino acid changes in 5 of 17 positions between codons 80 and 96, while cluster II had differences resulting in amino acid changes in 6 of 8 positions between codons 112 to 119 (Fig. 4B).

Hybrid viruses were constructed to further delineate the NIa sequences involved in the V20 infection phenotype. As convenient restriction sites were unavailable between the *Bam*HI and *Bsu*36I sites of TEV-GUS cDNA, a chimeric PCR strategy was adopted to generate hybrids with various amounts of TEV-

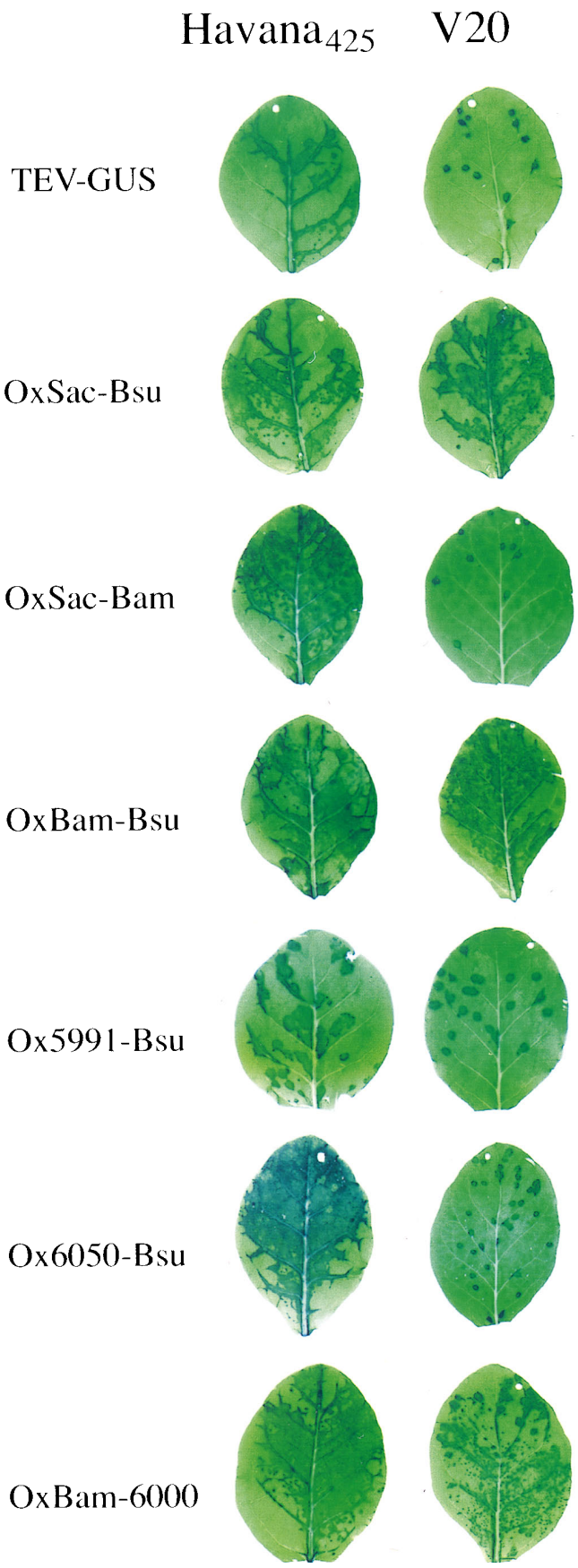

TABLE 1. Relative amplification of chimeric virus genomes in protoplasts

Virus	Mean relative amplification ± SD (n = 6)[a]		Systemic infection in V20
	$Havana_{425}$	V20	
TEV-GUS	100.0	100.0	−
TEV-GUS/VNN[b]	0.0 ± 0.0	0.0 ± 0.0	ND[c]
$TEV\text{-}GUS^{OxSac\text{-}Bsu}$	28.8 ± 22.5	22.4 ± 7.5	+
$TEV\text{-}GUS^{OxSac\text{-}Bam}$	48.8 ± 12.5	51.6 ± 31.3	−
$TEV\text{-}GUS^{OxBam\text{-}Bsu}$	17.9 ± 15.5	13.7 ± 6.2	+
$TEV\text{-}GUS^{Ox5991\text{-}Bsu}$	22.4 ± 8.8	20.4 ± 4.8	−
$TEV\text{-}GUS^{Ox6050\text{-}Bsu}$	91.6 ± 28.5	181 ± 14.0	−
$TEV\text{-}GUS^{OxBam\text{-}6244}$	16.8 ± 14.0	15.2 ± 3.4	+
$TEV\text{-}GUS^{OxBam\text{-}6069}$	32.4 ± 17.9	30.5 ± 9.4	+
$TEV\text{-}GUS^{OxBam\text{-}6000}$	32.8 ± 22.5	25.6 ± 7.6	+

[a] Level at 72 h p.i., using parental TEV-GUS level as the 100% standard.
[b] Contains a mutation affecting NIb polymerase and was included as a negative control for genome amplification.
[c] ND, not determined.

Oxnard sequence within this region (Fig. 5A). Each chimeric virus was given a superscript designation indicating the nucleotide position or restriction site delineating the 5′ and 3′ borders of the TEV-Oxnard sequence. Chimeric viruses containing TEV-Oxnard 5′ endpoints at NIa codon 101 ($TEV\text{-}GUS^{Ox5991\text{-}Bsu}$) or codon 120 ($TEV\text{-}GUS^{Ox6050\text{-}Bsu}$) and 3′ endpoints at the *Bsu*36I site within the proteinase domain coding region were constructed to test the effects of substituting TEV-Oxnard cluster I or TEV-Oxnard clusters I and II, respectively (Fig. 5A). Both $TEV\text{-}GUS^{Ox5991\text{-}Bsu}$ and $TEV\text{-}GUS^{Ox6050\text{-}Bsu}$ were capable of systemic infection of $Havana_{425}$ plants (Fig. 5B, columns 4 and 5), but neither was able to systemically infect V20 plants (Fig. 5D, columns 4 and 5). In inoculated V20 leaves, both $TEV\text{-}GUS^{Ox5991\text{-}Bsu}$ and $TEV\text{-}GUS^{Ox6050\text{-}Bsu}$ were restricted to isolated infection foci with little or no vasculature-mediated spread (Fig. 3). These results indicate that sequence included within TEV-Oxnard cluster I is necessary for systemic infection of V20 plants. Curiously, $TEV\text{-}GUS^{Ox5991\text{-}Bsu}$ consistently yielded GUS activity in upper leaves of $Havana_{425}$ plants at levels that were nearly 100-fold lower than that in parental TEV-GUS-infected $Havana_{425}$ plants (Fig. 5B, column 4). Differential accumulation of parental TEV-GUS and $TEV\text{-}GUS^{Ox5991\text{-}Bsu}$ was not observed, however, in *N. tabacum* cv. Xanthi nc plants (Fig. 5C).

An additional series of hybrids containing TEV-Oxnard 5′ endpoints at the *Bam*HI site and 3′ endpoints at codons 185 ($TEV\text{-}GUS^{OxBam\text{-}6244}$), 132 ($TEV\text{-}GUS^{OxBam\text{-}6069}$), and 104 ($TEV\text{-}GUS^{OxBam\text{-}6000}$) was also analyzed (Fig. 5A). Each of these viruses was able to infect both $Havana_{425}$ and V20 plants systemically (Fig. 5B and D, columns 6 to 8). Inoculated leaves from both V20 and $Havana_{425}$ leaves containing each of these three chimeric viruses exhibited vasculature-associated distribution patterns (Fig. 3 and data not shown). As the 67-nucleotide cluster I sequence was the only TEV-Oxnard sequence common to all hybrid viruses able to infect V20 systemically, it was concluded that this segment contains a determinant sufficient to account for the TEV-Oxnard phenotype.

To verify that the phenotypes of the five PCR-generated hybrid viruses in $Havana_{425}$ and V20 plants were not

FIG. 3. In situ analysis of chimeric TEV-GUS-infected $Havana_{425}$ and V20 plants. Histochemical localization of GUS activity was performed in inoculated leaves of $Havana_{425}$ (left column) and V20 (right column) plants at 7 days p.i.

A

```
                                                                  BamHI
OX    1 GGAAGAAGAATCAGAAGCACAAGCTTAAGATGAGAGGGGCGCGTGAAGCTAGAGGGCAA
HAT   1 .....................................A........GG............

OX   61 TATGAGGTTGCGGCGGACCCAGAGGCGCTAGAACATTACTTTGGAAGTGCATATAATAAC
HAT  61 ...........A.....G.............................C............

OX  121 AGAGGAAGGCGCAAGGGCACCACGAGAGGAATGGGTGCAAAATCTCGGAAATTCATAATC
HAT 121 .A.....A.................................G................A.

                                                       BamHI
OX  181 ATGTATGGGTTTGATCCAACTGATTTTTCATACATTATGTTTGTGGATCCCTTGACACGT
HAT 181 .....................................G............A......G..

OX  241 CACACTATTGACGAGTCCACACCCGCATCCATGGATTTAGTGCAGGATGAGTTTGGGAAG
HAT 241 ...........T.........AA....C.T..T............C..........A...

OX  301 GTTAGAACACGCATGTTAATTGACGATGAGATAGATTCTCAAAATCTTAAAGCCAACACC
HAT 301 ...................................GC......G.....GCA..C.....

OX  361 ACAATCCATGCTTATTTGGTGAATAGTGGCACGAAGAAAGTTCTGAAGGTTGATTTGACA
HAT 361 ............................................T...........A...

OX  421 CCACATTCGTCGCTGCGTGCGAGTGAGAGATCAACAGCAATAATGGGATTTCCTGAAAGG
HAT 421 .....C........A.............A...............................

OX  481 GAGAACGAACTGCGTCAAACCGGCATGGCAGTGCCAGTGGCTTATGATCAATTGCCACCA
HAT 481 .....T...T..................................................

OX  541 AAGAATGAGGACTTGACGCTTGAAGGAGAAAGCTTGTTTAAGGGACCACGTGATTACAAC
HAT 541 ..................T.........................................

OX  601 CCGATATCGAGTGCCATTTGTCATTTGACGAATGAATCTGAGGGGCACACAACATCGTTG
HAT 601 ...........CA............................T..................

OX  661 TATGGTATTGGTTTTGGTCCTTTCATCATAACAAACAAGCACTTGTTTAGAAGAAATAAT
HAT 661 ...........A........C........T..............................

OX  721 GGAACACTGTCAGTCCAATCACTACATGGTGTATTCAAGGTCAAGAACACCACAACTTTG
HAT 721 ..........TG.........................................G......

                                                  Bsu36I
OX  781 CAACAGCATCTCATTGATGGGAGGGACATGATGCTTATTCGCATGCCTAAG
HAT 781 .....A..C.......................AA...........
```

B

```
OX    1 GKKNQKHKLKMRGAREARGQYEVAADPEALEHYFGSAYNNRGRRKGTTRGMGAKSRKFII
HAT   1 ............E..G.........E..............K.K................N

                         (BamHI)           I                          II
OX   61 MYGFDPTDFSYIMFVDPLTRHTIDESTPASMDLVQDEFGKVRTRMLIDDEIDSQNLKANT
HAT  61 ............R......G.......N.PI....H...............EP.S.STH.

OX  121 TIHAYLVNSGTKKVLKVDLTPHSSLRASERSTAIMGFPERENELRQTGMAVPVAYDQLPP
HAT 121 .............................K..............................

          VPg       Pro
         Domain ↓ Domain
OX  181 KNEDLTLEGESLFKGPRDYNPISSAICHLTNESEGHTTSLYGIGFGPFIITNKHLFRRNN
HAT 181 ......F.................T........D..........................

OX  241 GTLSVQSLHGVFKVKNTTTLQQHLIDGRDMMLIRMPK
HAT 241 ...L..........................II.....
```

FIG. 4. (A) Nucleotide and deduced amino acid sequences of part of TEV-Oxnard NIa. Nucleotide sequence of the first 825 nucleotides of TEV-Oxnard NIa (OX) was compared with the corresponding TEV-HAT NIa sequence (HAT). Dots indicate identical nucleotides. The *Bam*HI and *Bsu*36I restriction sites are indicated. (B) Deduced amino acid sequence for the first 825 nucleotides of TEV-Oxnard compared with the corresponding TEV-HAT NIa sequence. Dots indicate identical amino acids. Two clusters of amino acid sequence are indicated and labeled I and II. The arrow indicates the internal cleavage site separating the VPg domain from the proteinase domain.

due to indirect effects on replication, genome amplification of each virus was measured in Havana$_{425}$ and V20 protoplasts. Four of the five hybrid genomes (TEV-GUS$^{Ox5991\text{-}Bsu}$, TEV-GUS$^{OxBam\text{-}6244}$, TEV-GUS$^{OxBam\text{-}6069}$, and TEV-GUS$^{OxBam\text{-}6000}$) amplified to levels reaching only 15.2 to 32.8% of that of parental TEV-GUS. Each genome amplified to similar levels in both types of protoplasts (Table 1). As TEV-GUS$^{OxBam\text{-}6244}$, TEV-GUS$^{OxBam\text{-}6069}$, and TEV-GUS$^{OxBam\text{-}6000}$ were able to systemically infect V20 plants but TEV-GUS$^{Ox5991\text{-}Bsu}$ was not, these data suggest that long-distance movement activity was not a direct function of amplification levels. One hybrid virus (TEV-GUS$^{Ox6050\text{-}Bsu}$) amplified to 91.6% of the level of parental virus in Havana$_{425}$ protoplasts and to nearly twice the parental level in V20 protoplasts (Table 1). However, this virus was unable to infect V20 systemically, again indicating a lack of correlation between amplification level in protoplasts and V20 infection phenotype in plants.

Coinfection of Havana$_{425}$ and V20 plants. The restriction of long-distance movement of TEV-HAT-derived strains in V20 plants could be due to a defense response elicited upon infection. This putative response, however, would not involve hypersensitivity, as no visible reactions were detected in inocu-

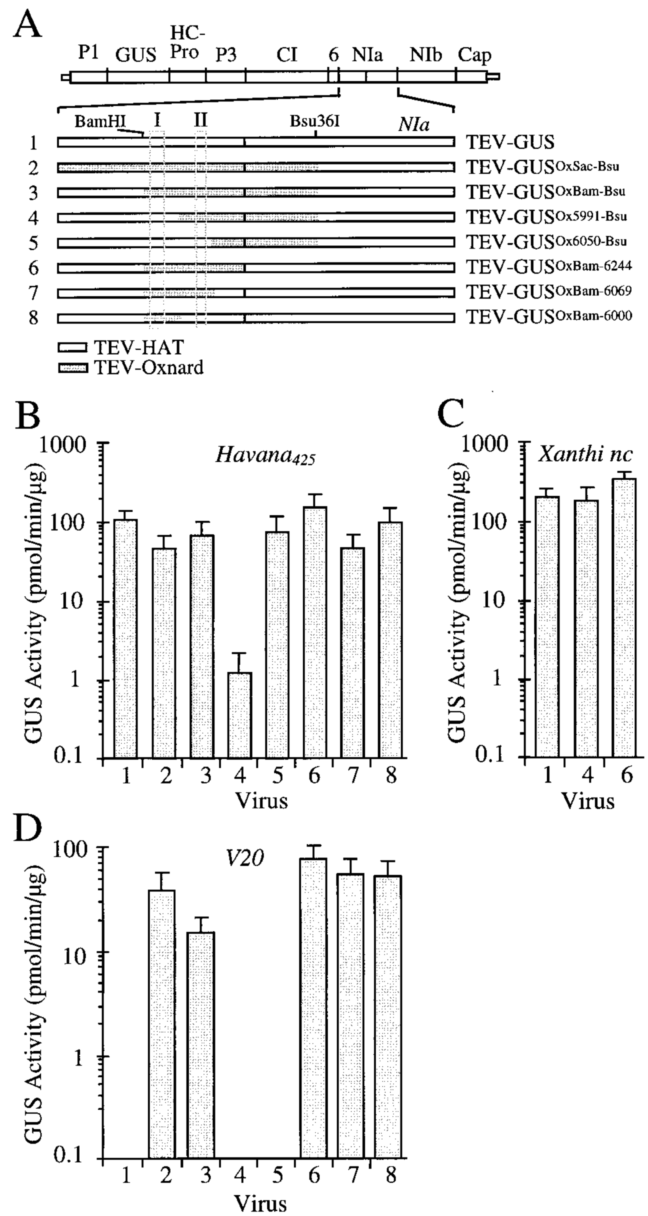

FIG. 5. (A) Diagrammatic representation of chimeric TEV genomes. Vertical boxes delineate locations of clusters I and II as shown in Fig. 4B. (B to D) Systemic infection of Havana$_{425}$ (B), Xanthi nc (C), and V20 (D). The number under each bar corresponds to the code for each virus as shown in panel A. GUS activity was quantitated in 2+ leaves at 7 days p.i. Each bar represents the mean ± standard deviation from eight plants. Note that the scale of the *y* axis in panels B to D was adjusted to provide the best relative comparison of data within each panel.

TABLE 2. Analysis of TEV-GFP and TEV-GUS$^{OxBam\text{-}Bsu}$ in coinoculation experiments

Virus(s)	Plant	Inoculated leaves (7 days p.i.)[a]		Upper, noninoculated leaves (7 days p.i.)			
		TEV-GFP foci	TEV-GUS$^{OxBam\text{-}Bsu}$ foci	GFP fluorescence[b]	TEV-GFP PCR[c]	GUS activity[d] (pmol/min/μg of protein)	TEV-GUS$^{OxBam\text{-}Bsu}$ PCR[c]
None	Havana$_{425}$	0	NT[e]	−	−	0	−
TEV-GUS$^{OxBam\text{-}Bsu}$	Havana$_{425}$	0	Confluent[f]	−	−	241 ± 77	+
TEV-GFP	Havana$_{425}$	Confluent	0	+++	+	0.6 ± 0.1	−
TEV-GUS$^{OxBam\text{-}Bsu}$ and TEV-GFP	Havana$_{425}$	Confluent	Confluent	+++	+	1.5 ± 1.3	+
None	V20	0	NT	−	−	0	−
TEV-GUS$^{OxBam\text{-}Bsu}$	V20	0	Confluent	−	−	119 ± 81	+
TEV-GFP	V20	113 ± 53	0	+/−	+	0.4 ± 0.1	−
TEV-GUS$^{OxBam\text{-}Bsu}$ and TEV-GFP	V20	40 ± 10	Confluent	−	−	122 ± 36	+

[a] TEV-GFP foci were counted in inoculated leaves of 10 plants, using a long-wave (365-nm) UV lamp (model UVL-21; UVP, Inc., San Gabriel, Calif.). TEV-GUS$^{OxBam\text{-}Bsu}$ foci were counted after infiltration of leaves with a GUS histochemical substrate.

[b] Detected qualitatively on upper, noninoculated leaves (1+, 2+, and 3+) in 10 plants, using a long-wave (365-nm) UV lamp. −, no fluorescence; +/−, isolated fluorescent spots on some plants; +++, systemic fluorescence pattern.

[c] Reverse transcription-PCR was performed by using RNA from 3+ leaves with primers that annealed within P1 and HC-Pro coding regions. TEV-GFP and TEV-GUS$^{OxBam\text{-}Bsu}$-derived PCR products were distinguished by size in agarose gel electrophoresis.

[d] Measured in 2+ leaves.

[e] NT, not tested.

[f] Foci were confluent after vascular spread.

lated leaves. If TEV-HAT-derived strains elicited a long-distance movement-limiting defense response, it was predicted that this response might also restrict TEV-GUS$^{OxBam\text{-}Bsu}$ in coinfection experiments. As shown above, the TEV-GUS$^{OxBam\text{-}Bsu}$ strain was capable of systemic movement in single-infection assays in V20 plants. The TEV-GFP strain was derived solely from the TEV-HAT strain, but it encodes green fluorescent protein (GFP) as a reporter. In preliminary experiments, TEV-GFP was shown to exhibit a restricted infection phenotype similar to those of other TEV-HAT-derived strains (e.g., TEV-GUS) in V20 plants. Isolated, fluorescent infection foci were visible with little or no vasculature-associated spread in inoculated V20 leaves (Table 2 and data not shown). In inoculated leaves of Havana$_{425}$, extensive TEV-GFP-induced fluorescence was visible along major and minor veins (Table 2 and data not shown). In upper, noninoculated leaves V20 plants, GFP fluorescence indicative of systemic infection typically was not observed, although in some experiments, isolated spots with GFP fluorescence were occasionally detected. In upper leaves of Havana$_{425}$, GFP fluorescence was uniformly distributed. The infection phenotypes of TEV-GFP and TEV-GUS in V20 plants, therefore, were similar.

As a test of the induced defense model, Havana$_{425}$ and V20 plants were coinfected with TEV-GUS$^{OxBam\text{-}Bsu}$ and TEV-GFP. The titers of TEV-GUS$^{OxBam\text{-}Bsu}$ and TEV-GFP in these inocula were normalized after bioassay using Xanthi nc plants such that 250 to 300 focus-forming units were applied to each inoculated leaf. The extent of vasculature-associated and systemic infection by TEV-GUS$^{OxBam\text{-}Bsu}$ in single and dual infections was analyzed in inoculated and 2+ leaves of both Havana$_{425}$ and V20 plants. As shown above, single infections of either Havana$_{425}$ and V20 plants by TEV-GUS$^{OxBam\text{-}Bsu}$ yielded high levels of GUS activity in upper leaves (Table 2) and vasculature-associated spread in inoculated V20 leaves. In dual infections of Havana$_{425}$ plants, TEV-GFP-induced fluorescence in inoculated and upper, noninoculated leaves was similar to that in TEV-GFP single-infected plants, but TEV-GUS$^{OxBam\text{-}Bsu}$ in 2+ leaves was suppressed by over 100-fold (Table 2). All dual-inoculated Havana$_{425}$ plants were infected by TEV-GUS$^{OxBam\text{-}Bsu}$, as revealed by detection of GUS activity in all inoculated leaves (Table 2). No deletion variants lacking the GUS coding sequence were detected by PCR analysis of noninoculated Havana$_{425}$ leaves. In Havana$_{425}$ plants, therefore, it appeared that TEV-GFP interfered with establishment of systemic infection by TEV-GUS$^{OxBam\text{-}Bsu}$. In contrast, after dual infection of V20 plants, TEV-GUS$^{OxBam\text{-}Bsu}$ accumulated in 2+ leaves to the same level as it did in single-infected V20 plants (Table 2). Inoculated leaves of dual-infected V20 plants contained isolated TEV-GFP infection foci (40 ± 10 per leaf), as revealed by quantitation of fluorescent foci at 7 days p.i. (Table 2), indicating that the plants were infected by both viruses. These data suggest that coinfection of V20 plants by TEV-GUS$^{OxBam\text{-}Bsu}$ and TEV-GFP results in neither elicitation of a TEV-GUS$^{OxBam\text{-}Bsu}$-limiting defense response nor any measurable interference of TEV-GUS$^{OxBam\text{-}Bsu}$ systemic infection.

DISCUSSION

Two potyviral proteins, CP and HC-Pro, are known to be required for long-distance movement of TEV in susceptible hosts (9, 12, 13, 20). It is likely that the movement functions of CP involve direct interactions with the viral genome, in the context of either a virion or a nonvirion ribonucleoprotein complex. The role of HC-Pro in long-distance movement is not clear, although recent studies suggest that HC-Pro may stimulate long-distance movement through an indirect effect on one or more host processes (20). It was logical, therefore, to test the hypothesis that the restriction of long-distance movement of TEV-HAT-derived strains in V20 tobacco was due to incompatibility between CP and/or HC-Pro and the host. However, the recombinant genome strategy used in these experiments failed to provide support for this hypothesis, indicating that CP and HC-Pro are not directly involved in the host-specific interactions governing V20 infection phenotype.

Rather, the TEV genetic determinant controlling long-distance movement phenotype in V20 was located within a 67-nucleotide segment spanning codons 78 to 99 for the VPg

domain of the NIa polyprotein. This sequence from TEV-Oxnard, when transferred to the homologous position in TEV-HAT-derived strains, was sufficient to convert a restricted strain into a strain competent to move long distances in V20 plants. The 67-nucleotide interval contains the sequences coding for cluster I amino acid residues, which have relatively high variability between the two strains. The VPg domain is required for genome replication, presumably as a primer during initiation of RNA synthesis, and remains covalently attached to viral RNA through a phosphoester linkage with Tyr62 (31–33, 38). The VPg domain also contains a nuclear localization signal within the sequence between residues 40 and 49 (5, 38). Therefore, assuming that the V20 infection phenotype is due to an activity of the protein rather than the RNA coding sequence, the VPg domain of NIa contains information specifying at least three functions: initiation of RNA synthesis, subcellular transport, and host-specific long-distance movement.

Virus derived from one recombinant genome, TEV-GUS$^{Ox5991\text{-}Bsu}$, displayed a novel systemic infection phenotype. In addition to lacking long-distance movement capability in V20 plants, this virus accumulated to nearly 100-fold-lower levels than did parental TEV-GUS in Havana$_{425}$ plants. In Xanthi nc plants, however, TEV-GUS$^{Ox5991\text{-}Bsu}$ accumulated to the same levels as the parental virus. This virus contains cluster I sequence from TEV-HAT and cluster II sequence from TEV-Oxnard. It is suggested that this combination of TEV-Oxnard and TEV-HAT sequences resulted in a VPg domain with incompatibilities in both V20 and Havana$_{425}$ plants but not Xanthi nc plants. This result further implicates this region of the TEV genome as a critical determinant in virus-host interactions that facilitate systemic infection.

As the VPg domain provides a critical function during TEV RNA synthesis, it was possible that the TEV-Oxnard-derived strains were competent for long-distance movement in V20 because they replicate to higher levels than do TEV-HAT-derived strains. However, the data do not support this hypothesis. Most of the recombinant viruses containing TEV-Oxnard sequences encoding part of NIa within a TEV-HAT genetic background amplified to lower levels than did the parental virus in both Havana$_{425}$ and V20 protoplasts, regardless of whether the recombinant strain was competent for long-distance movement in V20. There was no correlation between long-distance movement activity in V20 plants and enhanced relative amplification in V20 protoplasts. Each recombinant strain with a suppressed amplification phenotype in protoplasts contained either or both of clusters I and II from the NIa sequence of TEV-Oxnard. The one recombinant strain (TEV-GUS$^{Ox6050\text{-}Bsu}$) that amplified as well as parental virus in Havana$_{425}$ and V20 protoplasts contained both cluster I and cluster II sequences from TEV-HAT. The suppressed amplification levels of the recombinant strains may have been the result of slight incompatibilities between the cluster I-II region of TEV-Oxnard NIa and one or more other TEV-HAT replication proteins. Alternatively, the recombinant NIa molecules may have had moderate folding defects, lower stability, or lower intrinsic activity. In any case, it is clear that the long-distance movement phenotype and genome amplification phenotype in V20 plants and protoplasts, respectively, are independent characteristics.

In mechanistic terms, how might the VPg domain condition host genotype-specific long-distance movement in a genome replication-independent manner? Two possibilities should be considered. First, the VPg domain may be involved directly in movement of TEV from leaf to leaf. The fact that long-distance movement is selectively affected by the V20 genotype, which appears to be a function of two unlinked recessive loci (37), could indicate that the VPg domain interacts with host factors specifically involved in long-distance movement. However, the VPg domain might be necessary for both cell-to-cell movement and long-distance movement, but long-distance movement is the only process affected by the two host loci identified in V20 plants. If the VPg domain participates directly as a movement protein, it may function in the context of a covalent protein-RNA complex, as each new TEV genome contains a VPg domain (or full-length NIa) attached to the 5′ terminus (6, 32, 36, 39). This raises the intriguing possibility that TEV movement involves a 5′-to-3′ vectorial transfer of genomes, either as ribonucleoproteins or as virions, through plasmodesmata. In fact, this would not be the only example of facilitated nucleic acid transport involving a covalent association with protein specifying targeting information in plant cells. Transfer of T-DNA through nuclear pores during *Agrobacterium tumefaciens* infection occurs in the context of a protein-DNA complex containing covalently linked VirD2 and noncovalently associated VirE2 proteins, each of which possesses a nuclear localization signal (40). Second, the VPg domain could serve as an elicitor of a long-distance movement-restricting defense response. In this scenario, the TEV-HAT-derived VPg would elicit a defense response specifically in V20 plants, whereas TEV-Oxnard-derived VPg would not. If selective induction of a defense response accounts for the infection phenotypes observed, the nature of such a response is not clear. Visible reactions, such as a hypersensitive response, are not evident in inoculated leaves containing TEV-HAT-derived strains. Further, the coinfection experiments revealed that TEV-HAT-derived strains do not induce a generalized defense response capable of limiting TEV-Oxnard-derived strains.

Finally, it is intriguing to consider that a growing body of evidence lends support to the general view that plant viral replication proteins participate in virus-host interactions that condition systemic or restricted infection phenotypes. Several examples of studies using mutational and recombinant genome strategies where restricted movement phenotypes are conditioned by genes encoding RNA-dependent RNA polymerase or helicase-like proteins have been documented (reviewed in reference 7). Whether these types of virus-host interactions influence movement directly or indirectly, such as through induction or suppression of defense responses, and whether viral replication proteins are involved in coupling between genome synthesis and intercellular movement remain to be determined.

ACKNOWLEDGMENTS

We thank Aaron Unterbrink for assistance with growth of plants.

This research was supported by grants from the NIH (AI27832) and the USDA National Research Initiative Program (95-37303-1867) to J.C.C. and a National Research Service Award from NIH (AI09121) to M.C.S.

REFERENCES

1. **Allison, R., R. E. Johnston, and W. G. Dougherty.** 1986. The nucleotide sequence of the coding region of tobacco etch virus genomic RNA: evidence for the synthesis of a single polyprotein. Virology **154:**9–20.
2. **Atreya, C. D., and T. P. Pirone.** 1993. Mutational analysis of the helper component-proteinase gene of a potyvirus: effects of amino acid substitutions, deletions, and gene replacement on virulence and aphid transmissibility. Proc. Natl. Acad. Sci. USA **90:**11919–11923.
3. **Bradford, M. M.** 1976. A rapid and sensitive method for the quantitation of microgram quantities of protein utilizing the principle of protein-dye binding. Anal. Biochem. **72:**248–254.
4. **Callaway, A., W. Liu, V. Andrianov, L. Stenzler, J. Zhao, S. Wettlaufer, P. Jayakumar, and S. H. Howell.** 1996. Characterization of cauliflower mosaic virus (CaMV) resistance in virus-resistant ecotypes of Arabidopsis. Mol. Plant-Microbe Interact. **9:**810–818.

4a. **Carrington, J. C., P. E. Jensen, and M. C. Schaad.** Genetic evidence for an essential role for potyvirus CI protein in cell-to-cell movement. Submitted for publication.
5. **Carrington, J. C., D. D. Freed, and A. J. Leinicke.** 1991. Bipartite signal sequence mediates nuclear translocation of the plant potyviral NIa protein. Plant Cell **3:**953–962.
6. **Carrington, J. C., R. Haldeman, V. V. Dolja, and M. A. Restrepo-Hartwig.** 1993. Internal cleavage and *trans*-proteolytic activities of the VPg-proteinase (NIa) of tobacco etch potyvirus in vivo. J. Virol. **67:**6995–7000.
7. **Carrington, J. C., K. D. Kasschau, S. K. Mahajan, and M. C. Schaad.** 1996. Cell-to-cell and long-distance movement of viruses in plants. Plant Cell **8:**1669–1681.
8. **Christie, S. R., D. E. Purcifull, and C. E. Dean.** 1974. Resistance in V 20 tobacco to tobacco etch virus. Plant Dis. Rep. **58:**658–659.
9. **Cronin, S., J. Verchot, R. Haldeman-Cahill, M. C. Schaad, and J. C. Carrington.** 1995. Long-distance movement factor: a transport function of the potyvirus helper component-proteinase. Plant Cell **7:**549–559.
10. **Deom, C. M., M. Lapidot, and R. N. Beachy.** 1992. Plant virus movement proteins. Cell **69:**221–224.
11. **Ding, X. S., M. H. Shintaku, S. A. Arnold, and R. S. Nelson.** 1995. Accumulation of mild and severe strains of tobacco mosaic virus in minor veins of tobacco. Mol. Plant-Microbe Interact. **8:**32–40.
12. **Dolja, V. V., R. Haldeman, N. L. Robertson, W. G. Dougherty, and J. C. Carrington.** 1994. Distinct functions of capsid protein in assembly and movement of tobacco etch potyvirus in plants. EMBO J. **13:**1482–1491.
13. **Dolja, V. V., R. Haldeman-Cahill, A. E. Montgomery, K. A. VandenBosch, and J. C. Carrington.** 1995. Capsid protein determinants involved in cell-to-cell and long distance movement of tobacco etch potyvirus. Virology **207:** 1007–1016.
14. **Dolja, V. V., H. J. McBride, and J. C. Carrington.** 1992. Tagging of plant potyvirus replication and movement by insertion of β-glucuronidase into the viral polyprotein. Proc. Natl. Acad. Sci. USA **89:**10208–10212.
15. **Gal-On, A., I. Kaplan, M. J. Roossinck, and P. Palukaitis.** 1994. The kinetics of infection of zucchini squash by cucumber mosaic virus indicate a function for RNA 1 in virus movement. Virology **205:**280–289.
16. **Goodrick, B. J., C. W. Kuhn, and R. S. Hussey.** 1991. Restricted systemic movement of cowpea chlorotic mottle virus in soybean with nonnecrotic resistance. Phytopathology **81:**1426–1431.
17. **Holt, C. A., R. A. J. Hodgson, F. A. Coker, R. N. Beachy, and R. S. Nelson.** 1990. Characterization of the masked strain of tobacco mosaic virus: identification of the region responsible for symptom attenuation by analysis of an infectious cDNA clone. Mol. Plant-Microbe Interact. **3:**417–423.
18. **Horton, R. M.** 1995. PCR-mediated recombination and mutagenesis. Mol. Biotechnol. **3:**93–99.
19. **Kasschau, K. D., and J. C. Carrington.** 1995. Requirement for HC-Pro processing during genome amplification of tobacco etch potyvirus. Virology **209:**268–273.
20. **Kasschau, K. D., S. Cronin, and J. C. Carrington.** 1997. Genome amplification and long-distance movement functions associated with the central domain of tobacco etch potyvirus helper component-proteinase. Virology **228:**251–262.
21. **Klein, P. G., R. R. Klein, E. Rodríguez-Cerezo, A. G. Hunt, and J. G. Shaw.** 1994. Mutational analysis of the tobacco vein mottling virus genome. Virology **204:**759–769.
22. **Kunkel, T. A., J. D. Roberts, and R. Zakour.** 1987. Rapid and efficient site-specific mutagenesis without phenotypic selection. Methods Enzymol. **154:**367–382.
23. **Lee, S., D. C. Stenger, D. M. Bisaro, and K. R. Davis.** 1994. Identification of loci in *Arabidopsis* that confer resistance to geminivirus infection. Plant J. **6:**525–535.
24. **Leisner, S. M., and R. Turgeon.** 1993. Movement of virus and photoassimilate in the phloem: a comparative analysis. Bioessays **15:**741–748.
25. **Leisner, S. M., R. Turgeon, and S. H. Howell.** 1993. Effects of host plant development and genetic determinants on the long-distance movement of cauliflower mosaic virus in Arabidopsis. Plant Cell **5:**191–202.
26. **Li, X. H., and J. C. Carrington.** 1995. Complementation of tobacco etch potyvirus mutants by active RNA polymerase expressed in transgenic cells. Proc. Natl. Acad. Sci. USA **92:**457–461.
27. **Lucas, W. J., and R. L. Gilbertson.** 1994. Plasmodesmata in relation to viral movement within leaf tissues. Annu. Rev. Phytopathol. **32:**387–411.
28. **Mahajan, S., V. V. Dolja, and J. C. Carrington.** 1996. Roles of the sequence encoding tobacco etch virus capsid protein in genome amplification: requirements for the translation process and a *cis*-active element. J. Virol. **70:**4370–4379.
29. **Meshi, T., F. Motoyoshi, T. Maeda, S. Yashiwoka, H. Watanabe, and Y. Okada.** 1989. Mutations in the tobacco mosaic virus 30-kD protein gene overcome Tm-2 resistance in tomato. Plant Cell **1:**512–522.
30. **Motoyoshi, F., and N. Oshima.** 1977. Expression of genetically controlled resistance to tobacco mosaic virus infection in isolated tomato leaf mesophyll protoplasts. J. Gen. Virol. **34:**499–506.
31. **Murphy, J. F., P. G. Klein, A. G. Hunt, and J. G. Shaw.** 1996. Replacement of the tyrosine residue that links a potyviral VPg to the viral RNA is lethal. Virology **220:**535–538.
32. **Murphy, J. F., R. E. Rhoads, A. G. Hunt, and J. G. Shaw.** 1990. The VPg of tobacco etch virus RNA is the 49 kDa proteinase or the N-terminal 24 kDa part of the proteinase. Virology **178:**285–288.
33. **Murphy, J. F., W. Rychlik, R. E. Rhoads, A. G. Hunt, and J. G. Shaw.** 1990. A tyrosine residue in the small nuclear inclusion protein of tobacco vein mottling virus links the VPg to the viral RNA. J. Virol. **65:**511–513.
34. **Negrutiu, I., R. Shillito, I. Potrykus, G. Biasini, and F. Sala.** 1987. Hybrid genes in the analysis of transformation conditions. 1. Setting up a simple method for direct gene transfer in plant protoplasts. Plant Mol. Biol. **8:**363–373.
35. **Nelson, R. S., G. Li, R. A. J. Hodgson, R. N. Beachy, and M. Shintaku.** 1993. Impeded phloem-dependent accumulation of the masked strain of tobacco mosaic virus. Mol. Plant-Microbe Interact. **6:**45–54.
36. **Riechmann, J. L., S. Laín, and J. A. García.** 1989. The genome-linked protein and 5′ end RNA sequence of plum pox potyvirus. J. Gen. Virol. **70:**2785–2789.
37. **Schaad, M. C., and J. C. Carrington.** 1996. Suppression of long-distance movement of tobacco etch virus in a nonsusceptible host. J. Virol. **70:**2556–2561.
38. **Schaad, M. C., R. Haldeman-Cahill, S. Cronin, and J. C. Carrington.** 1996. Analysis of the VPg-Proteinase (NIa) encoded by tobacco etch potyvirus: effects of mutations on subcellular transport, proteolytic processing, and genome amplification. J. Virol. **70:**7039–7048.
39. **Shahabuddin, M., J. G. Shaw, and R. E. Rhoads.** 1988. Mapping of the tobacco vein mottling virus VPg cistron. Virology **163:**635–637.
40. **Sheng, J., and V. Citovsky.** 1996. Agrobacterium-plant cell DNA transport: have virulence proteins, will travel. Plant Cell **8:**1699–1710.
41. **Simon, A. E., X. H. Li, J. E. Lew, R. Stange, C. Zhang, M. Polacco, and C. D. Carpenter.** 1992. Susceptibility and resistance of *Arabidopsis thaliana* to turnip crinkle virus. Mol. Plant-Microbe Interact. **5:**496–503.
42. **Thompson, J. D., D. G. Higgins, and T. J. Gibson.** 1994. CLUSTAL W: improving the sensitivity of progressive multiple sequence alignment through sequence weighting, position-specific gap penalties and weight matrix choice. Nucleic Acids Res. **22:**4673–4680.
43. **Traynor, P., B. M. Young, and P. Ahlquist.** 1991. Deletion analysis of brome mosaic virus 2a protein: effects on RNA replication and systemic spread. J. Virol. **65:**2807–2815.
44. **Weber, H., S. Schultze, and A. J. P. Pfitzner.** 1993. Two amino acid substitutions in the tomato mosaic virus 30-kilodalton movement protein confer the ability to overcome the *Tm-2*^{2} resistance gene in tomato. J. Virol. **67:** 6432–6438.